R-peak Detection in Electrocardiogram Signals Using Continuous Wavelet Transform

Seyed Reza Razavi, Mohammad Hossein Doost Mohammadi*

Department of Electrical Engineering
Hamedan University of Technology
Shahid Fahmide Ave, Mardom St., Hamedan, Iran
E-mails: seyy_razavi@elec.iust.ac.ir, doost.mohammadi@hut.ac.ir

Corresponding author

Received: March 23, 2016 **Accepted: December 14, 2016**

Published: June 30, 2017

Abstract: *In this paper, an efficient wavelet-based method is proposed to detect the R-peak from QRS complex. At first, a preprocessing step is taken to remove high frequency noise of electrocardiogram (ECG) data. Then, continuous wavelet transform (CWT) is applied to the signal and the R-peaks of QRS complexes are detected with acceptable accuracy using special thresholding method. The detection performance of the proposed algorithm is evaluated against the MIT-BIH Arrhythmia Database. The numerical results indicated that the proposed method achieved a detection rate of 99.72% over all standard database used for evaluation. Also, evaluating the performance of the proposed algorithm on ECG signal with poor signal quality indicated the reliability of this algorithm even under the condition of poor SNR. Finally, the accuracy of detection rate is proven by comparing the proposed algorithm with some other methods from different literatures.*

Keywords: *QRS complex, R-peak detection, Electrocardiogram, Continuous wavelet transform, Denoising.*

Introduction

In today's world, the problem of population aging, and the consequent age-related health issues, has created a strong demand for more convenient health-care solutions. One of the solutions widely used today is telemedicine, which allows professionals to monitor the health status of vulnerable seniors and patients with heart diseases remotely. In this technique, different tools such as telephone line, mobile network and satellite networks are used as telecommunication platforms. One of the most vital signs that needs to be monitored is electrocardiogram signal (ECG). This sign is transmitted via telemedicine [14].

ECG signal is an electrical signal generated by heart's cardiac muscle during contraction and expansion. This signal provides the electrical activity and the status of the patient's heart in any given instant. In a typical signal, three waveforms can be seen in every heartbeat: P-wave, waveform QRS, and T-curve [7, 22]. A typical ECG signal and its important features are shown in Fig. 1. The feature extraction algorithms can be categorized into two main groups [29]: (1) Transform-based algorithms [2, 4, 23, 30]; (2) Wave-form or morphology based algorithms [15]. Transform-based algorithms take place in wavelet and frequency domain, in which frequency-based methods including the Discrete Fourier Transform and Discrete Cosine Transform are applied.

The QRS complex is one of the most important components to be extracted from an ECG signal. For example, since the accuracy of instantaneous heart period estimation relies on the performance of QRS detection, so detection of QRS complex provides a significant basis for instantaneous Heart Rate (HR) computation. It should be noted that ECG signals are varying with the variation of subjects and also affected by various noises such as baseline drifts, electrode motion noise or power – line interference noise [5, 6, 21]. For better QRS detection, ECG signal need to be noise-free.

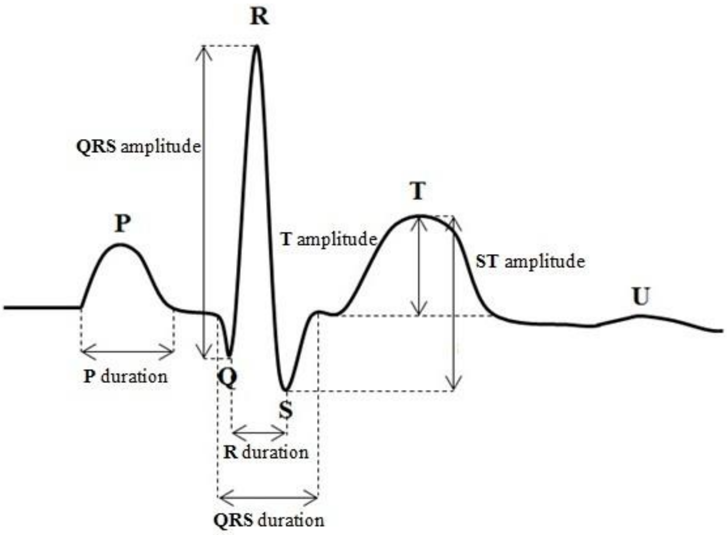

Fig. 1 ECG signal and its morphology parameters

To date, many approaches have been proposed to detect QRS complex and, specifically, the R-peak of the signal. Some of the algorithms are developed based on digital filters [21, 25, 27], while some are based on nonlinear transforms [26, 28]. In some methods, a specific QRS template is used to prevent detection algorithm from being degraded by undesired noise sources [12, 13, 33]. Some works have been done based on adaptive thresholding method [10]. Also, some review article has been presented about various QRS detection algorithms [11].

One of the most widely used methods is based on continuous and discrete wavelet transforms, a technique that has been considerably progressed in recent years [1, 16, 18, 20, 24, 34, 35]. Most of these methods were developed based on a discrete wavelet transform (DWT). But in this paper, an improved algorithm based on the continuous wavelet transform (CWT) is proposed to detect the QRS complex, especially R-peak. In this algorithm, CWT is used with the help of some thresholding methods [16, 34] to achieve improved results with reasonable accuracy in detection of the R-peak. The improved performance of the proposed algorithm is proven by comparing with other algorithms presented in previous works [3, 9, 16, 21, 27, 32, 35].

This paper is organized as follows: In Section 2, the construction of a CWT and choosing the appropriate wavelet is introduced briefly. Section 3 deals with the presentation of proposed algorithm. The results of the proposed algorithm are presented in Section 4, as well as accuracy comparison with various algorithms, together with a discussion of the advantages of the proposed algorithm. Finally in Section 5, a brief conclusion of this study is presented.

Wavelet transform background

Continuous wavelet transform

As described in the wavelet literature [8, 17], the continuous wavelet transform of a continuous square – integral function of $x(t)$ is mathematically defined as follows:

$$CWT_x^{\psi}(a\,,b) = \frac{1}{\sqrt{|a|}} \int_{-\infty}^{+\infty} x(t)\psi^*\left(\frac{t-b}{a}\right), \tag{1}$$

where b and a are the translation and scale parameters, respectively, and $\psi(t)$ is a continuous function in both time and frequency domain, which is the so-called mother wavelet. Word mother is used because all the shifted and scaled versions are obtained from the basic function called the mother wavelet. In scientific expression, the mother wavelet is a function template to generate all other wavelets by time shifting and dilation operation of wavelet transform. Using continuous wavelet transform provides a thorough analysis of any change in the signal frequency; on the other hand, and as a drawback, it results in increase in data size and higher processing time.

According to [8, 17], when using CWT, the high frequency components of the signal are reflected at small scales and the low frequency components of the signal are reflected at large scales. Also, continuous wavelet transform is able to characterize the local regularity of signal by decomposing the ECG into elementary building blocks that are well localized both in time and frequency window [34].

Choosing the type of wavelet

Selecting the type of wavelet plays an important role in signal analysis and its results. But overall, there is no absolute method for choosing a particular wavelet. Due to the nature and the shape of ECG signals, some types of wavelets, such as Daubechies, Symlet, and Bi-orthogonal, are more efficient to use for analysis of these signals.

In this paper, Daubechies2 wavelet (db2) is used which is structurally similar to the QRS and given the fact that a continuous wavelet transform is used, this kind of wavelet, highlights the R-peak to be easily separated from the other features of the ECG signal. Scaling function and wavelet function of Daubechies2 wavelet is shown in Fig. 2.

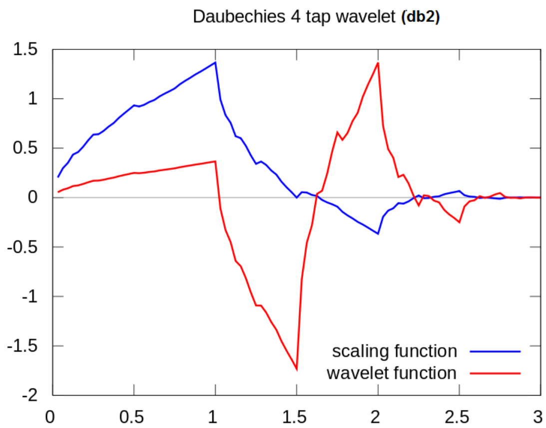

Fig. 2 Scaling function and wavelet function of Daubechies2 wavelet [31]

Methodology

In this section, the methodology of the proposed algorithm is fully described. For simplicity, the algorithm is divided into several sub-stages and the respective process of each sub-stage is carefully expressed. The flowchart of the proposed algorithm is shown in Fig. 3. The algorithm consists of some stages such as pre-processing, applying continuous wavelet transform, thresholding, and R-peak extraction. There are some types of noise inherent in the data collection process. Therefore, a preprocessing stage is needed (as a sub-stage) to eliminate the noise as much as possible. In the next stage, CWT is applied to the preprocessed signals. Then, the obtained wavelet coefficients are thresholded and the R-peak will be extracted. In the following, the stages of the proposed algorithm will be described.

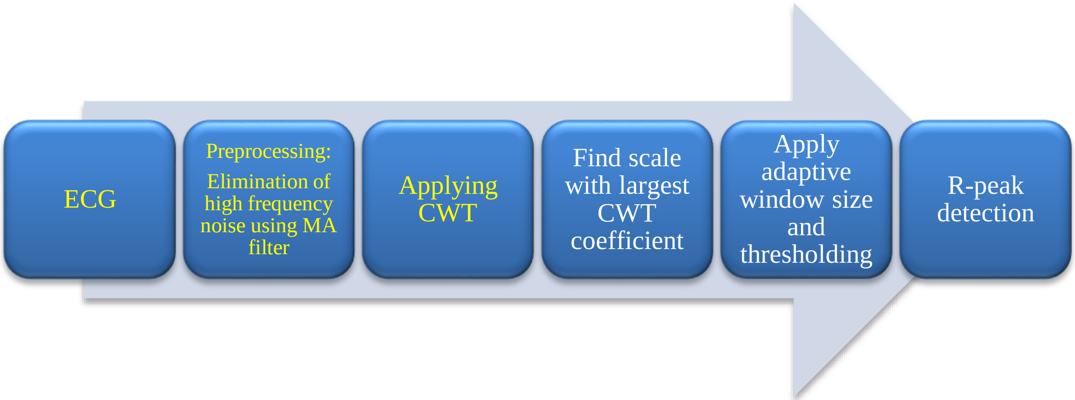

Fig. 3 A block diagram of the R-peak detection algorithm

Preprocessing

The first stage of the proposed algorithm is preprocessing shown as a second block of Fig. 3. As mentioned before, there are some types of noise inherent in the data collection process. The main sources of such artifacts are: (1) low frequency noise such as the baseline drift, and (2) high-frequency noise, such as the electromyographic (EMG) noise or power – line interference noise. High frequency noise is going to be removed in this stage while low frequency noise will be eliminated in CWT stage.

In this stage, the method proposed by Zhang and Lian [34] is used to reduce the noise level (such as EMG noise or power – line interference noise) from the ECG signal and prepare it for the rest of the algorithm. In this method, a three points moving average filter is used to realize the low pass filter and makes the signal smoother. It is calculated from:

$$y(t) = \frac{1}{6}[f(t-1) + 4f(t) + f(t+1)]. \tag{2}$$

Applying CWT

After preprocessing, a continuous wavelet transform is applied to the filtered signal. By applying the continuous wavelet transform, different coefficients will appear from scaling and transferring of mother wavelet. The relationship between the scales and frequency of the original signal is such that the lower scales contain the high frequency components of the original signal and the higher scales contain the low frequency components. The result of applying CWT on ECG signals is shown in Fig. 4 and Fig. 5 using scales 32 and 64, respectively. All simulations have been performed in *Matlab*® software using the *Wavelab* toolbox [31].

As it is shown in Fig. 4 and Fig. 5, and by considering the results obtained in [7, 14], the QRS complex is located on the lower scale, so according to [14], the scales of 1 to 32 is used for CWT. Low frequency noises appear in higher scales of the wavelet transform, but by choosing a scale of 1 to 32, this noise would be limited. As a result, one of the great advantages of the CWT is that it eliminates low frequency noise by itself and there would be no demand for further filtering method.

So far, there are some scales which contain the frequency properties of QRS complex. Now, we need to choose an appropriate scale to apply threshold. To do this, location of the largest coefficient is found through the total coefficients and its scale is considered. This scale contains the biggest amount of energy of the ECG signal. Then, overall this scale is separated from the rest of CWT coefficients. The separated coefficients in a vector form contain QRS complex. In the next step, this vector should be thresholded to detect the R-peak which is described in the next section.

Thresholding and R-peak detection

To identify the R-peak, the separated vector from the CWT coefficients should be thresholded, so the R-peak can be extracted from them. In this paper, for thresholding and R-peak detection, the method presented in [16] is used in which, the adaptive window size is used to detect the R-peak. Speaking of the window, it has a length of 0.5 seconds, and it moves 0.1 seconds each time to detect the next R-peak. Then, the maximum signal on each applied window can be calculated and if this maximum value was found in the location of 0.15 up to 0.35 seconds of window length and if it was bigger than the threshold, it could be considered as a location of QRS complex.

Here is the method to calculate the threshold: the position of maximum value (i) in the window is adopted. Then another maximum of the CWT coefficients vector is calculated from the beginning of the window location up to 5 seconds after. Then, to apply a threshold and for the nest detection, the second maximum value α is multiplied by various coefficients. This could be defined as follow:

$$thr\ (i) = \alpha \max\big(ym(i - s{:}\, i)\big). \tag{3}$$

It can be found from [21] that the error rate of this method is still too high. So in order to reduce the error rate, two thresholds are used instead. To apply the second threshold, the average value of the last 8 RR intervals is considered as a reference. It can be described as follow [16]:

$$RR[n] = \tfrac{1}{8}\textstyle\sum_{a=1}^{8} RR[n-a]. \tag{4}$$

Now, if the distance of the last two detected R-peak is more than 1.5 times average RR interval, we will come back to the location of previous R-peak and perform the detection algorithm with second threshold. The threshold 1 is 0.35 times maximum peak, and the threshold 2 is 0.2 times the maximum peak. The last step is matching the positions of those extreme points to the denoised ECG signal, the position of maximum positive value is point R in the interval. The window size is 0.05 s before and after the extreme points.

Results and discussion

MIT-BIH database [19] is used to evaluate the performance of the proposed algorithm. The MIT-BIH Arrhythmia Database contains 48 half-hour excerpts of two-channel ambulatory ECG recordings, obtained from 47 subjects studied by the BIH Arrhythmia Laboratory between 1975 and 1979. Twenty-three recordings were chosen at random from a set of 4000 24-hour ambulatory ECG recordings collected from a mixed population of inpatients (about 60%) and outpatients (about 40%); the remaining 25 recordings were selected from the same set to include less common but clinically significant arrhythmias that would not be well-represented in a small random sample [19].

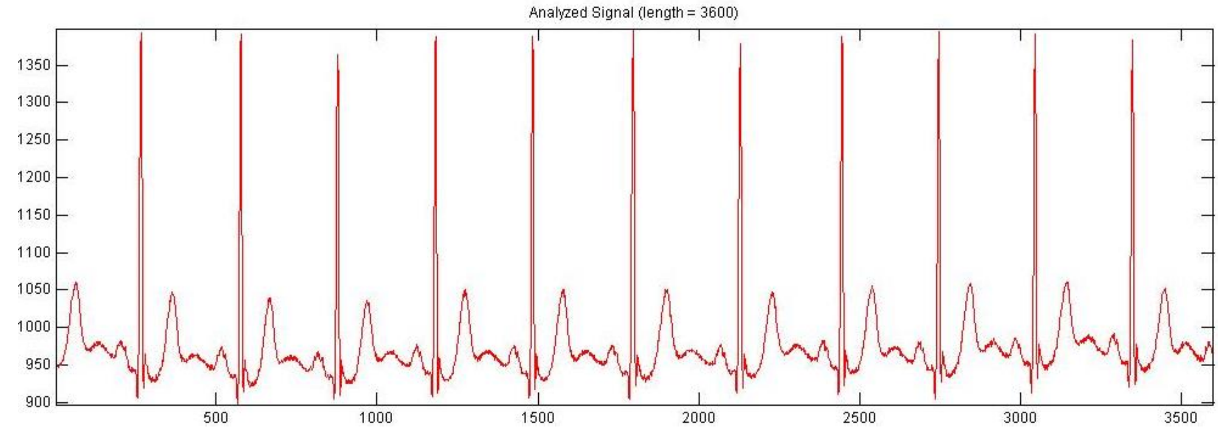

(a)

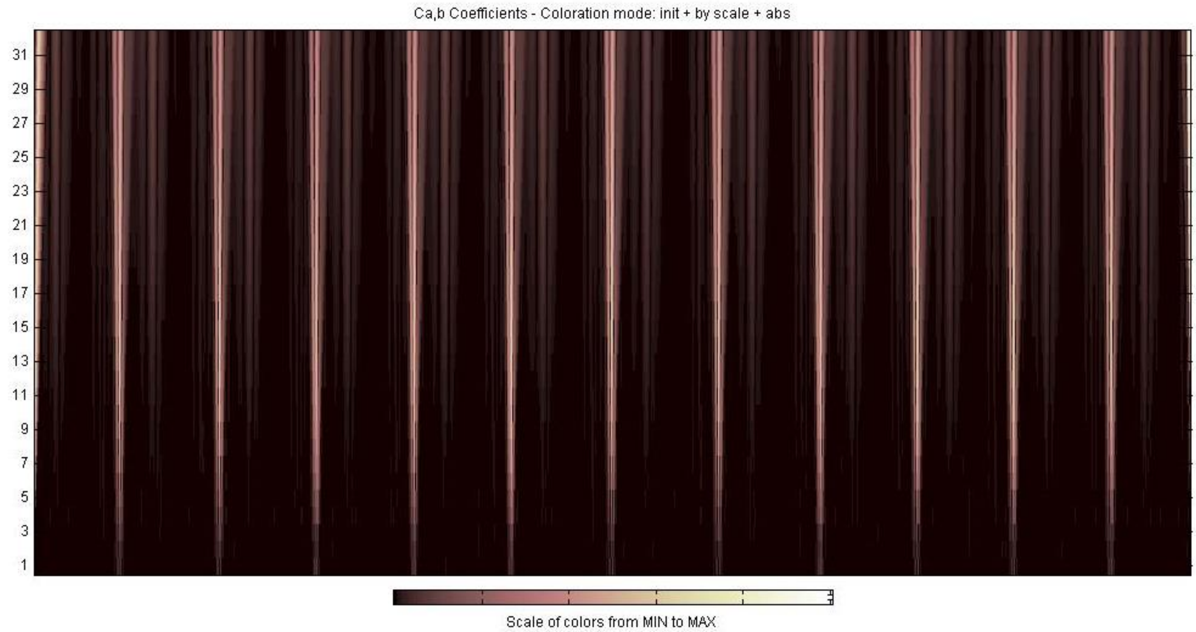

(b)

(c)

Fig. 4 ECG signal and its CWT coefficients: (a) record 103 of MIT-BIH database [19]; (b) its CWT coefficients for a scale range of 1 to 32; (c) coefficients line for scale a = 16.

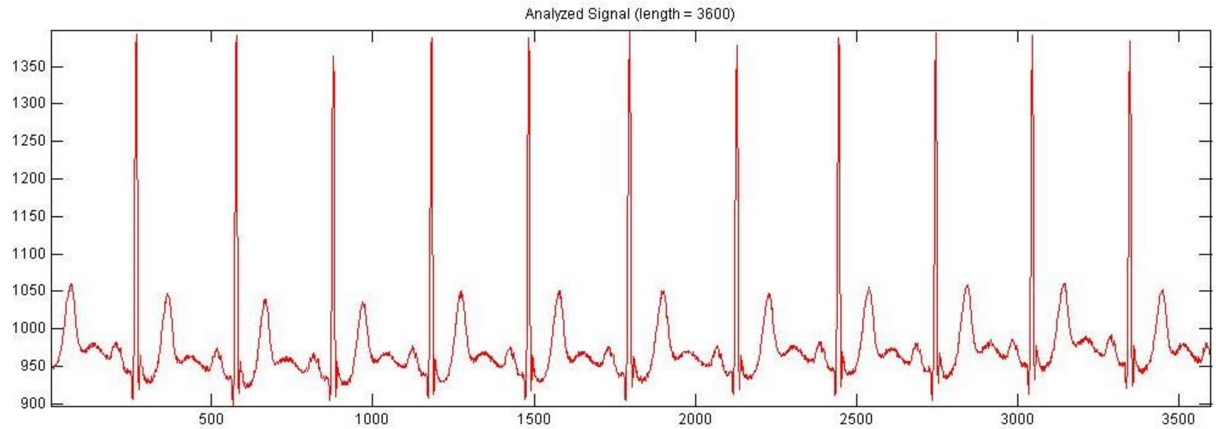

(a)

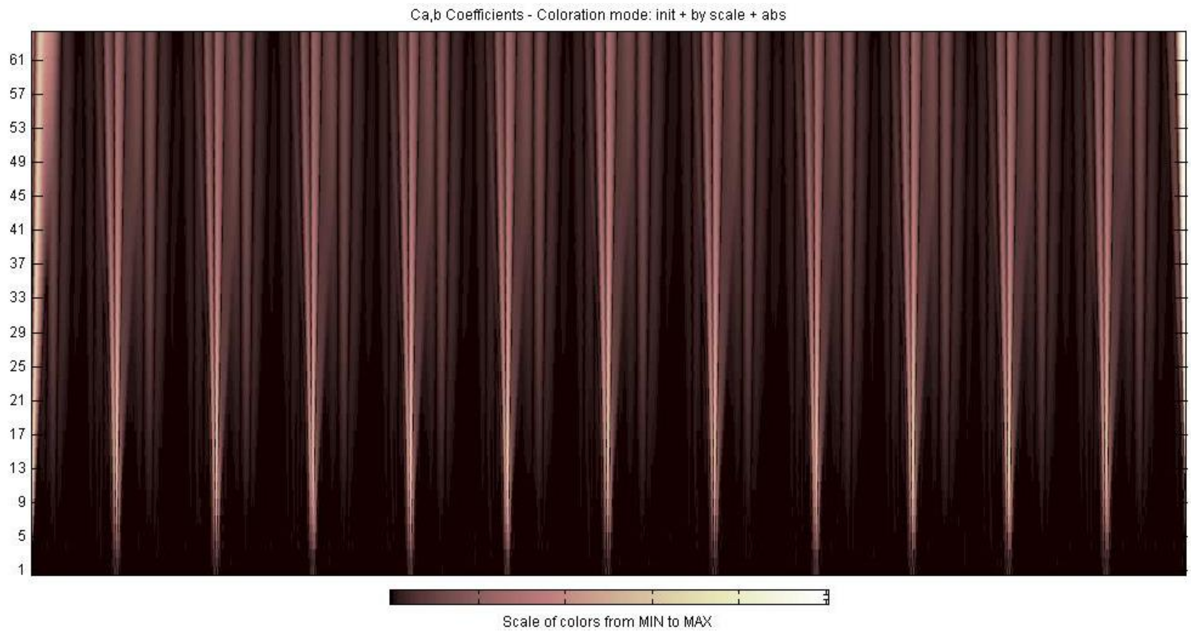

(b)

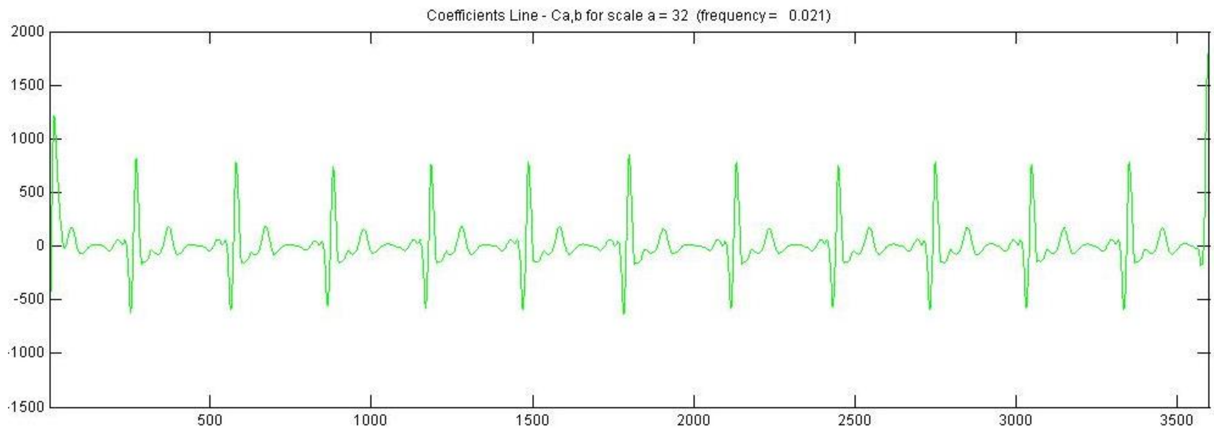

(c)

Fig. 5 ECG signal and its CWT coefficients: (a) record 103 of MIT-BIH database [19]; (b) its CWT coefficients for a scale range of 1 to 64; (c) coefficients line for scale a = 32.

The recordings were digitized at 360 samples per second per channel with 11-bit resolution over a 10 mV range. Two or more cardiologists independently annotated each record; disagreements were resolved to obtain the computer-readable reference annotations for each beat (approximately 110 000 annotations in all) included with the database [19].

In this work, the whole 30 min of each record was used for evaluation. Also, it should be mentioned that the first channel of each record was processed with the aim of comparing with other published works.

A typical PC using Windows 8 as its OS powered by a Pentium Core i7 processor (3GHz) was used to apply the proposed algorithm to the database and to do the whole computing process. All simulations have been performed in *Matlab*® software using the *Wavelab* toolbox [31]. A typical result of R-peak detection algorithm is shown in Fig. 6.

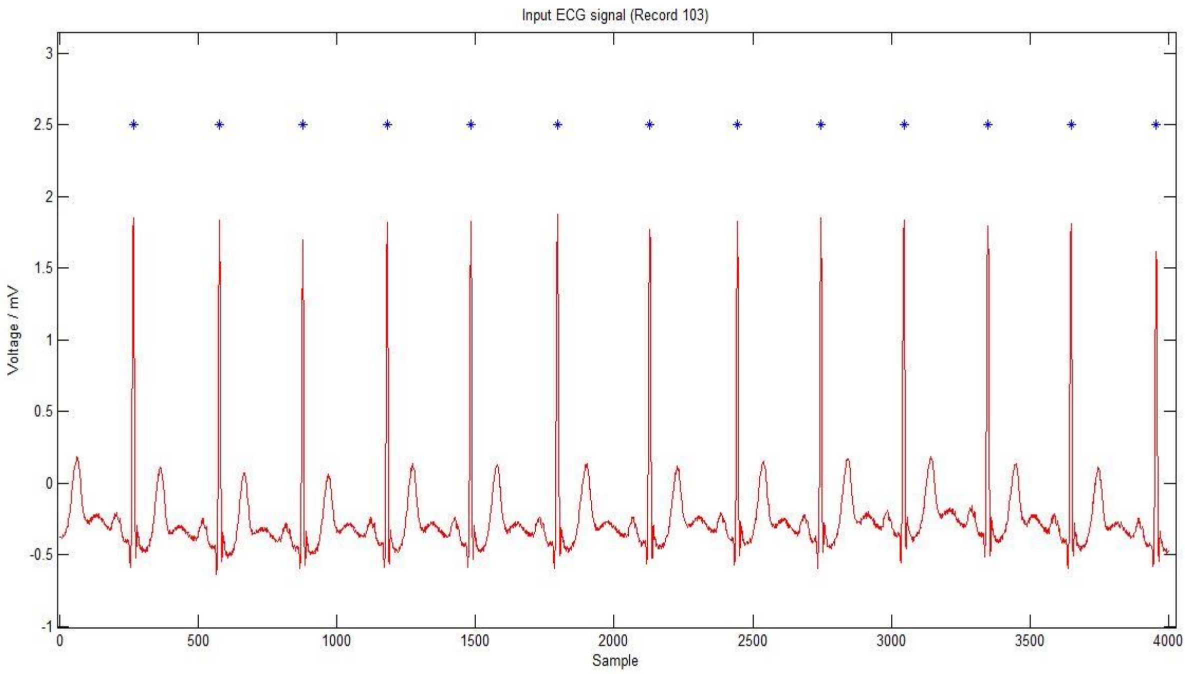

Fig. 6 Detection result of the proposed algorithm for record 103

In this session, two parameters are used in order to evaluate the actual performance of the proposed algorithm, which are called "sensitivity" and "positive predictivity" and defined as follows:

$$Se = \frac{TP}{TP+FN} \quad (sensitivity), \tag{5}$$

$$P^{+} = \frac{TP}{TP+FP} (positive\ predictivity), \tag{6}$$

where *FN* (False Negative Beat) is the number of peaks present in the original signal, but the algorithm does not identify them; and *FP* (False Positive Beat) is the number of peaks wrongly identified as R-peak by the algorithm. Also, *TP* (True Positive) is the total number of peaks that have been identified by the algorithm. Moreover, we used $\min(Se, P^{+})$ to simplify the presentation of overall detection rate achieved by algorithms [14]:

$$QRS\ detection\ rate\ (QRS\ DR) = \min(Se, P^{+}). \quad (7)$$

The results obtained after applying the proposed algorithm to the chosen database are presented in Table 1. As mentioned before, the mother wavelet used for the proposed algorithm was Daubechies 2. It is clear from Table 1 that the proposed algorithm produced 142 *false positive* (*FP*'s) in total, and 117 *false negative* (*FN*'s), and an overall correct detection rate of 99.71% is achieved.

It should be mentioned that for some records in database, modest detection results may be achieved. The reason may be the fact that these records are affected by the high noise levels. It means that the poor signal quality of records, i.e. very low SNR or high noise level, may cause the results of detection algorithms to be degraded. More details could be found at [12, 14, 18, 24, 35].

In order to find how noise affects the performance of detection algorithm, another numerical experiment was performed in this work. In this case, a noise free record was combined with a zero mean white Gaussian noise (WGN) with variance σ^2.This noise free record has been achieved by applying wavelet denoising to the record 103 in the MIT-BIH database. In this step, different values of noise variance σ^2 were determined by setting SNR between 0 dB to 30 dB.

The results of applying the proposed algorithm to the noisy record 103 with different SNR, are summarized in Table 2. As listed in Table 2, a QRS detection rate of 100% could be achieved at SNR equal to 13 dB. Also, good QRS detection rate still could be achieved at lower SNR down to 5 dB.

It should be mentioned that presence of many slow waves like PVC's in a record somehow might affect the accuracy of wavelet-based algorithms. It should be noticed that the proposed algorithm is customized to facilitate detecting the impulse-like QRS complexes rather the slow waves such as P or T-waves. Therefore, if the parameters of thresholding are fixed during the entire process, the proposed method may not always be able to accurately detect low amplitude and frequent PVC's; thus, the number of FN's might undesirably increase.

For instance, there is such problem in record 208 in which 53 FN has been detected. Although the proposed method showed an acceptable performance for other records with PVC's in the database, such as records 100, 109, 112, 119, 230 (with FN's 1, 4, 0, 0, 0, respectively). Therefore, it could be said that the weak results achieved for similar records should be attributed to either the limitation of the algorithm or the limitation of these data records themselves.

One solution could be manual adjustment of the thresholding parameters during the detection process, especially for the records with frequent PVC's. In addition, applying this algorithm to some signals with abnormal high amplitude T-peak, may lead to non-acceptable results. Therefore, the modest results for some records could be achieved due to limitation of the method as well as limitation of record itself [14].

Finally, the performance of the proposed algorithm is compared with other methods in different literature. The results of this comparison are presented in Table 3. As can be seen, the proposed algorithm has better detection accuracy against other methods. But it should be noted that fewer records or fewer total beats are used for the proposed algorithm. Hence, there is the possibility that the detection accuracy might be lower as the number of records increase.

Table 1. Results of performance evaluation for the proposed detection algorithm

Record	Total Beats	FN Beats	FP Beats	Se (%)	P^+ (%)	QRS DR
100	2273	1	1	99.96	99.96	99.96
101	1865	5	6	99.73	99.68	99.68
102	2187	3	3	99.86	99.86	99.86
103	2084	0	0	100	100	100
104	2229	22	4	99.01	99.82	99.01
105	2572	4	39	99.84	98.5	98.5
106	2027	1	53	99.95	97.45	97.45
107	2137	45	1	97.9	99.95	97.9
109	2532	4	0	99.84	100	99.84
111	2124	2	2	99.9	99.9	99.9
112	2539	0	0	100	100	100
113	1795	1	5	99.94	99.72	99.72
114	1879	0	2	100	99.89	99.89
115	1953	0	0	100	100	100
116	2412	20	16	99.17	99.34	99.17
117	1535	0	2	100	99.87	99.87
118	2278	0	0	100	100	100
119	1987	0	2	100	99.9	99.9
121	1863	2	0	99.89	100	99.89
122	2476	0	0	100	100	100
123	1518	0	2	100	99.87	99.87
124	1619	6	4	99.63	99.75	99.63
200	2601	1	0	99.96	100	99.96
201	1963	21	0	98.93	100	98.93
202	2136	2	0	99.90	100	99.90
203	2980	34	46	98.86	98.46	98.46
205	2656	6	6	99.77	99.79	99.77
208	2955	53	9	98.21	99.69	98.21
209	3005	0	0	100	100	100
210	2650	3	9	99.89	99.66	99.66
212	2748	0	2	100	99.93	99.93
213	3251	0	5	100	99.85	99.85
214	2265	8	2	99.65	99.91	99.65
215	3363	0	0	100	100	100
217	2208	3	1	99.86	99.95	99.86
219	2154	1	0	99.95	100	99.95
220	2048	1	0	99.92	100	99.92
221	2427	5	3	99.79	99.88	99.79
222	2483	2	3	99.92	99.88	99.88
223	2605	1	1	99.96	99.96	99.96
228	2053	6	29	99.73	98.66	98.66
230	2256	0	4	100	99.82	99.82
231	1571	3	5	99.8	99.68	99.68
232	1780	0	24	100	98.67	98.67
233	3079	5	3	99.84	99.9	99.84
234	2753	0	1	100	99.96	99.96
46 patients	**105874**	**271**	**299**	**99.74**	**99.72**	**99.72**

Table 2. SNR vs. QRS detection rate for the record 103 in the MIT-BIH database

SNR (dB)	Se (%)	P^+ (%)
0	96.40	61.97
1.00	98.99	66.10
2.00	99.42	71.75
3.00	99.81	77.00
4.00	99.86	82.48
5.00	100.00	90.86
6.00	100.00	94.55
7.00	100.00	97.16
8.00	100.00	98.91
9.00	100.00	99.81
10.00	100.00	99.86
11.00	100.00	99.90
12.00	100.00	99.95
13.00	100.00	100.00
14.00	100.00	100.00
15.00	100.00	100.00
16.00	100.00	100.00
17.00	100.00	100.00
18.00	100.00	100.00
19.00	100.00	100.00
20.00	100.00	100.00
21.00	100.00	100.00
22.00	100.00	100.00
23.00	100.00	100.00
24.00	100.00	100.00
25.00	100.00	100.00
26.00	100.00	100.00
27.00	100.00	100.00
28.00	100.00	100.00
29.00	100.00	100.00
30.00	100.00	100.00

Table 3. Comparison of detection accuracy between the proposed algorithm and the algorithms of other literatures

Method	Total Beats	FN	FP	Se (%)	P^+ (%)	QRS DR
[3]	109453	354	405	99.68	99.63	99.63
[9]	102654	459	529	99.55	99.49	99.49
[16]	107634	324	379	99.70	99.65	99.65
[21]	116137	277	507	99.76	99.56	99.56
[27]	109510	1123	3981	90.05	86.46	86.46
[32]	97794	195	411	99.80	99.58	99.58
[35]	109494	393	193	99.64	99.82	99.64
Proposed Algorithm	**105874**	**271**	**299**	**99.74**	**99.72**	**99.72**

Conclusion

In this paper, a new wavelet-based method is introduced to detect QRS complex with a focus on the R-peak parameter. At first, a preprocessing is performed on the signal to remove its high frequency noises and to prepare it for applying CWT. In the next step, the continuous wavelet transform is used and its corresponding coefficients are calculated. By using a certain thresholding technique, the R-peak is detected. After preprocessing and applying the proposed algorithm to a set of noise corrupted ECG data from standard database, almost all QRS complexes can be successfully and reliably detected using CWT and an improved thresholding method. The approached results also indicated that in the proposed algorithm, there might exist a degree of flexibility to select the parameter value as well as robustness over a wide range of noise contamination. Finally, comparing the proposed algorithm with some other methods from different literature proved the accuracy of detection rate of the new method. It should be noticed that the proposed method might not be appropriate for signals with a high T-wave, atrial flutter and others that produce large CWT coefficients.

Acknowledgement

The authors would like to thank the Profs. M. Khodabandeh and Dr. Majid Majzoubi for their valuable comments and suggestions which helped to enhance the quality of this paper. Also, the authors are grateful for the helpful suggestions and comments provided by the anonymous reviewers of this work.

References

1. Alavi S., M. Saadatmand-Tarzjan (2013). A New Combinatorial Algorithm for QRS Detection, 3rd International e-Conference on Computer and Knowledge Engineering, October 31-November 1, Mashhad, Iran, 1788-1791.
2. Al-Hamdani O., A. Chekima, J. Dargham, S. H. Salleh, F. Noman, H. Hussain, A. Ariff, A. Mohd Noor (2013). Multimodal Biometrics Based on Identification and Verification System, J Biomet Biostat, 4(2), 1-8.
3. Arzeno N. M., Z. D. Deng, C. S. Poon (2008). Analysis of First-derivative Based QRS Detection Algorithms, IEEE Trans Biomed Eng, 55(2), 478-484.
4. Belgacem N., F. Bereksi-Reguig (2012). Person Identification System Based on Electrocardiogram Signal Using LabVIEW, International Journal on Computer Science and Engineering, 4(6), 974-981.
5. Bhoi A. K., K. S. Sherpa (2014). QRS Complex Detection and Analysis of Cardiovascular Abnormalities: A Review, Int J Bioautomation, 18(3), 181-194.
6. Bhoi A. K., K. S. Sherpa, B. Khandelwal (2015). Classification Probability Analysis for Arrhythmia and Ischemia Using Frequency Domain Features of QRS Complex, Int J Bioautomation, 19(4), 531-542.
7. Biradar B., G. Patil, S. Telgane, S. G. Hiremath (2014). Wavelet Transform Based on QRS Detection Using Diodic Algorithm, International Journal of Research in Engineering and Technology, 3(3), 909-915.
8. Burrus C. S., R. A. Gopinath, H. Guo (1998). Introduction to Wavelets and Wavelet Transforms, Prentice Hall, Upper Saddle River, New Jersey, USA.
9. Chen S. W., H. C. Chen, H. L. Chan (2006). A Real Time QRS Detection Method Based on Moving – Average Incorporating with Wavelet, J Comput Meth Prog Bio, 82(3), 187-195.
10. Christov I. (2007). Assessment of the Performance of the Adaptive Thresholding Algorithm for QRS Detection with the Use of AHA Database, Int J Bioautomation, 6, 27-37.

11. Christov I., I. Jekova, V. Krasteva, I. Dotsinsky, T. Stoyanov (2009). Rhythm Analysis by Heartbeat Classification in the Electrocardiogram, Int J Bioautomation, 13(2), 84-96.
12. Cohen A., D. Landsberg (1983). Adaptive Real-time Wavelet Detection, IEEE Trans Biomed Eng, 30(6), 332-340.
13. Dobbs S. E., N. M. Schmitt, H. S. Ozemek (1984). QRS Detection by Template Matching Using Real-time Correlation on a Microcomputer, J Clin Eng, 9(3), 197-212.
14. Ercelebi E. (2004). Electrocardiogram Signals De-noising Using Lifting-based Discrete Wavelet Transform, J Comput Biol Med, 34, 479-493.
15. Labati R. D., R. Sassi, F. Scotti (2013). ECG Biometric Recognition: Permanence Analysis of QRS Signals for 24 Hours Continuous Authentication, IEEE Workshop on Information Forensics and Security, November 18-21, Guangzhou, China, 31-36.
16. Lin H. Y., S. Y. Liang, Y. L. Ho, Y. H. Lin, H. Pin (2013). Discrete Wavelet Transform-based Noise Reduction and R-wave Detection for ECG Signals, IEEE 15th International Conference e-Health Networking, Applications & Services, October 9-12, Lisbon, Portugal, 355-360.
17. Mallat S. (2008). A Wavelet Tour of Signal Processing. 3rd Ed., Academic Press.
18. May C., N. Hubing, A. W. Hahn (1997). Wavelet Transforms for Electrocardiogram Processing, Biomed Sci Instrum, 33, 1-6.
19. MIT-BIH Arrythmia Database (1992). 2nd Ed., Cambridge, MA Massachusetts Institute of Technology, Biomedical Engineering Center, available from http://www.physionet.org/physiobank/database/html/mitdbdir/mitdbdir.htm (Last accessed May 15, 2017).
20. Mukherjee A., K. K. Ghosh (2013). A Noise Independent Approach to QRS-complex Detection Using CWT, International Conference on Informatics, Electronics & Vision, May 17-18, Dhaka, Bangladesh, 1-5.
21. Pan J., J. W. Tompkins (1985). A Real-time QRS Detection Algorithm, IEEE Trans Biomed Eng, 32(3), 230-236.
22. Sasikala P., R. S. D. Wahidabanu (2010). Identification of Individuals Using Electrocardiogram B, International Journal of Computer Science and Network Security, 12(10), 147-153.
23. Sharma R., T. Fatima, S. Anwarul, Srivastava D. (2013). Electrocardiogram Based Authentication System Using Video Streams, Proc. of Int Conf on Advances in Computer Science and Application, 753-758.
24. Sumathi S., M. Y. Sanavullah (2009). Comparative Study of QRS Complex Detection in ECG Based on Discrete Wavelet Transform, Int J Recent Trends in Engineering, 2(5), 273-277.
25. Sun Y., S. Suppappola, T. A. Wrublewski (1992). Microcontroller-based Real-time QRS Detection, Biomed Instrum Technol, 26(6), 477-484.
26. Suppappola S., Y. Sun (1994). Nonlinear Transform of ECG Signals for Digital QRS Detection: A Quantitative Analysis, IEEE Trans Biomed Eng, 41(4), 397-400.
27. Tanev S. (2012). Ventricular Beat Detection and Classification in Long Term ECG Recordings, Int J Bioautomation, 16(4), 273-290.
28. Trahanias P. E. (1993). An Approach to QRS Complex Detection Using Mathematical Morphology, IEEE Trans Biomed Eng, 40(2), 201-205.
29. Tseng K. K., J. Luo, R. Hegarty, W. Wang, D. Haiting (2014). Sparse Matrix for ECG Identification with Two-lead Features, The Scientific World Journal, 3(15), 1-9.
30. Wan Y., J. Yao (2008). A Neural Network to Identify Human Subjects with Electrocardiogram Signals, World Congress on Engineering and Computer Science, October 22-24, San Francisco, USA, 13-16.

31. Wavelab toolbox for MATLAB Software (n.d.), Retrieved August 15, 2015, http://www.statweb.stanford.edu/~wavelab
32. Xiaomeng C. (2011). A New Real-time ECG R-wave Detection Algorithm, 6th International Forum on Strategic Technology, August 22-24, Harbin, China, 1252-1255.
33. Xue Q., Y. H. Hu, W. J. Tompkins (1992). Neural-network-based Adaptive Matched Filtering for QRS Detection, IEEE Trans Biomed Eng, 39(4), 317-329.
34. Zhang F., Y. Lian (2007). Novel QRS Detection by CWT for ECG Sensor, Biomedical Circuits and System Conference, November 27-30, Montreal, Canada, 211-214.
35. Zidelmal Z., A. Amirou, M. Adnane, A. Belouchrani (2012). QRS Detection Based on Wavelet Coefficients, J Comput Meth Prog Bio, 107(3), 490-496.

Seyed Reza Razavi, B.Sc.
E-mail: seyy_razavi@elec.iust.ac.ir

Seyed Reza Razavi graduated as B.Sc. from the Faculty of Electronics, Hamedan University of Technology, in 2014. Since 2014 he is with the Centre of Biomedical Engineering, Iran University of Science and Technology. His interests are in developing algorithms and systems for biomedical signal processing.

Mohammad Hossein Doost Mohammadi, M.Sc.
E-mail: doost.mohammadi@hut.ac.ir

M. H. Doost Mohammadi obtained his M.Sc. degree from the Faculty of Electrical Engineering, Iran University of Science and Technology. Since 2009, he has been a lecturer in Electrical Engineering. Since 2011, he is a lecturer with the Centres of Electrical and Biomedical Engineering, Hamedan University of Technology, Iran. His interests are mainly in the fields of digital signal processing and digital image processing and their implementation systems, especially FPGA.